REVIEW **Communicated by Mark Churchland**

Toward a Biomimetic Neural Circuit Model of Sensory-Motor Processing

Stephen G. Lisberger
lisberger@neuro.duke.edu
Department of Neurobiology, Duke University School of Medicine, Durham, NC 27710, U.S.A.

Computational models have been a mainstay of research on smooth pursuit eye movements in monkeys. Pursuit is a sensory-motor system that is driven by the visual motion of small targets. It creates a smooth eye movement that accelerates up to target speed and tracks the moving target essentially perfectly. In this review of my laboratory's research, I trace the development of computational models of pursuit eye movements from the early control-theory models to the most recent neural circuit models. I outline a combined experimental and computational plan to move the models to the next level. Finally, I explain why research on nonhuman primates is so critical to the development of the neural circuit models I think we need.

1 Introduction

What does it mean to understand how the brain works? I subscribe to Feynman's view: "What I cannot create I do not understand." When I create a biologically realistic model, then I can say that I understand how a neural system works. Yet computational models of the brain take many forms, meaning that I need to specify the level of biological realism that I expect. Of course, the model must reproduce the input-output relationship of the brain system on which it is based. But to reveal how the brain works, the model will need to have circuits with realistic architecture and model neurons that produce realistic firing rates during behavior. Further, it should reproduce both the first- and second-order statistics of neural firing: mean and variance of responses across trials, trial-by-trial "noise" correlations between neurons, and trial-by-trial "neuron-behavior" correlations between the variations in spiking and behavioral output.

The sensory-motor system I have studied for the past half century offers great promise for developing the kind of biomimetic model that I describe in the previous paragraph. Smooth pursuit eye movements provide a quantifiable sensory-motor behavior that is amenable to study in nonhuman primates (Fuchs, 1967). Pursuit is driven by visual inputs, namely, by the motion of a small spot or patch of dots, and it generates smooth eye

Neural Computation **35, 384–412** (2023)
https://doi.org/10.1162/neco_a_01516

movements that take the eye in the direction of target motion at very close to target speed. It is one of the few voluntary movements where the link between sensation and action is both direct and continuously observable. Among behavioral systems, pursuit is unusually amenable to quantitative examination because we can map the input-output relationship via different visual motion stimuli and uncover situations where the baseline input-output relationship must be modulated by internal processes. To analyze the behavior, we have devised many behavioral and stimulus regimes. By going beyond the simple and obvious strategy of simply having a monkey track a moving spot, we have revealed multiple components of pursuit behavior and mapped many of those components to specific regions of the pursuit circuit. It is rare, in monkeys and rodents, to be able to characterize fully an interesting and complex input-output relationship while also understanding how it is modulated by internal parameters.

The neural circuit for pursuit is largely known, though it is probably more complicated and convoluted than we think, and important gaps still exist. Neural recordings are available from many, but not all, nodes of the pursuit circuit. Recordings were made during pursuit, and to some degree during the more elaborated set of behavioral and stimulus regimes we have developed. In some key areas, the recordings include both first- and second-order statistics of neural firing, and therefore they provide the substrate for a biologically realistic model of the neural pursuit system. Thus, smooth pursuit eye movements afford a nearly unique opportunity to understand the neural basis of a voluntary behavior and how it is created millisecond by millisecond by sensory-motor pathways at the full circuit level.

Computational modeling has a long tradition in smooth pursuit eye movements (Robinson, Gordon, & Gordon, 1986; Krauzlis & Lisberger, 1989; Ringach, 1995; Churchland & Lisberger, 2001a; Orban de Xivry, Coppe, Blohm, & Lefevre, 2013; Egger & Lisberger, 2022). However, most models have been designed to account for behavioral phenomena without regard for the architecture of signal processing within the essential circuit. Also, most models have been designed to account for a single feature of pursuit or at most a small set of features. My contributions have been as guilty of wearing these blinders as have those from everyone else. In the meantime, knowledge has expanded about pursuit behavior, the computational components of the pursuit system, and their neural correlates (Lisberger, 2015). The evolution of knowledge creates the possibility to start on a path toward a computational neural circuit model of how one sensory-motor system works in a behaving animal.

Here, I explain the evolution of knowledge and models of smooth pursuit eye movements in the time from our contribution in the first issue of *Neural Computation* (Krauzlis & Lisberger, 1989) to the present. I focus unabashedly on the research from my own laboratory to explain how our knowledge has evolved over 33 years. At the end of the review, I outline what I see as the next steps in computational models of smooth pursuit eye

movements, including an explanation of how the predictions of future models might be tested through application of modern molecular approaches and recording with multicontact probes in behaving monkeys. Finally, I defend the choice to pursue this particular goal in monkeys, even in the face of remarkable technological advances for neuroscience research on rodents.

2 Image Motion Models

The model we published in the first issue of *Neural Computation* (Krauzlis & Lisberger, 1989) had the singular goal of showing how the dynamics of visual motion processing could account for the dynamics of eye velocity as a function of time during pursuit. Earlier in the 1980s, we had rediscovered the step-ramp target motion of Rashbass (1961) and deployed it to analyze the initiation and steady state of pursuit (Lisberger & Westbrook, 1985). Briefly, the monkey fixates a stationary target that undergoes an instantaneous step of displacement and starts to move in a smooth ramp at a randomized time (see Figure 1A, top set of traces). Rashbass (1961) adjusted the size of the target step to show that pursuit responds to target motion while saccades respond to target offsets. We set the size of the target step to compensate for pursuit latency and largely eliminate saccades, thus revealing the dynamics of eye velocity at pursuit initiation (bottom set of traces). Under these conditions, the visual stimulus is a pulse of image velocity that ramps down as eye velocity increases (blue trace), and a brief interval of image deceleration during eye acceleration (red trace).

Our model deviated qualitatively from previous models of pursuit, which had focused on image velocity as input to the system and had placed most of the dynamics of pursuit in the motor system (Robinson et al., 1986). In our data, we found that the actual time-varying trajectory of pursuit eye velocity has two features that are not expected of a model based solely on image velocity. First, pursuit eye velocity settles at target velocity with little or no overshoot (see Figures 1A and 1C, black traces), while the latencies in the system mean that a model based on image velocity (see Figure 1C, red trace) shows considerable overshoot. Second, pursuit eye velocity sometimes oscillates at a fairly high frequency during steady-state tracking (see Figure 1C, black trace), while the image-velocity model predicts oscillations at a much lower frequency (see Figure 1C, green trace). The theoretical prediction is that an image velocity model should oscillate with a period that is four times the visual delay of 100 ms in our data (i.e., 2.5 Hz). In our data (see Figure 1C, red trace), steady-state pursuit oscillated at a frequency closer to 5 Hz (Goldreich, Krauzlis, & Lisberger, 1992).

We reproduced the actual trajectory of eye velocity during pursuit with an image-motion model (see Figure 1B) that includes much expanded visual motion processing. Here, visual motion processing is represented as the sum of (1) a traditional image velocity pathway, (2) a pathway that is sensitive only to the transient at the onset of motion, and (3) a pathway that

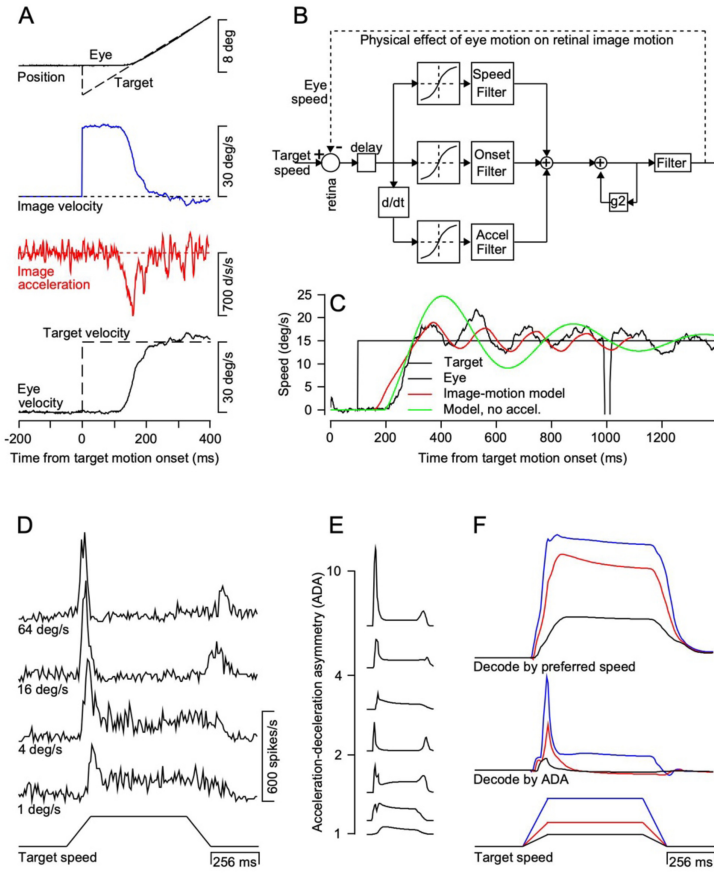

Figure 1: An image-motion model of pursuit. (A) Target and eye motion during a "step-ramp" target motion, showing the image velocity and accelerations that provide inputs for pursuit. (B) The original three-pathway, image-motion model. The "speed filter" is part of a pathway that is sensitive to image speed. The "onset filter" is part of a pathway that is sensitive only to the onset of motion. The "accel filter" is part of a pathway that is sensitive to smooth image acceleration. (C) Black, red, and green traces show typical eye velocity data and the predictions of the full image-motion model and the model without the acceleration pathway for a step of target speed from 0 to 15 deg/s. (D) Representative time-varying firing rates for an MT neuron during ramp increases and decreases in target speed in an anesthetized monkey. (E) Responses of model MT neurons with the same range of acceleration-deceleration asymmetry found in the data. (F) Decoded target speed and acceleration for a model population of MT neurons with a range of preferred speeds and acceleration-deceleration asymmetries. Figures are modified, with permission from Krauzlis and Lisberger (1989), Lisberger and Movshon (1999), and Lisberger (2015).

is sensitive to smooth image acceleration. The motor system is represented by a positive feedback pathway through gain element "g2" that sustains eye velocity during perfect tracking in the absence of image motion and renders image motion signals as commands for changes in eye velocity, that is, eye acceleration (Morris & Lisberger, 1987). The full image-motion model of Figure 1B predicts eye velocity (see Figure 1C, red trace) that nicely reproduces the two main features of actual eye velocity: (1) little overshoot and (2) oscillations of eye velocity at 5 Hz. The image acceleration pathway is essential for getting the correct frequency of oscillation, and a signal related to image deceleration (see the red trace in Figure 1A) is needed to prevent eye velocity overshoot after the initiation of pursuit.

It is possible to account for much of the trajectory of pursuit eye velocity with models that place the dynamics of the system in the motor pathways and rely on simple image velocity inputs to drive the model (Robinson et al., 1986; Ringach, 1995). However, these motor-dynamics models fail under a simple experimental manipulation that inserts delays of 20 to 100 ms into visual feedback (Goldreich et al., 1992). In experiments, the frequency of oscillation in steady-state tracking decreases gracefully as a function of visual delay. The same is true in image-motion models, but motor-dynamics models make more complicated and biologically unrealistic predictions (Churchland & Lisberger, 2001a). Thus, some of the dynamics of pursuit are caused by the properties of the full sensory-motor loop. Internal recurrent feedback loops drive other aspects of the dynamics, namely, the maintenance of accurate tracking in the absence of image motion across the retina during steady-state tracking. Perhaps this division of the labor of dynamics provides a simpler model system that offers lessons for the discussion for reaching movements of whether the dynamics in the motor cortex arise from internal recurrent circuits (Shenoy, Sahani, & Churchland, 2013) or from external sensory-motor loops (Kalidindi et al., 2021).

Models suggest experiments. The successful predictions of eye velocity from the image-motion model in Figure 1B inspired Tony Movshon and me to embark on extensive recordings from extrastriate visual area MT. Our goal was to look for neurophysiological evidence of the motion-onset or image-acceleration pathways in the image-motion model. Both lesion and microstimulation experiments show that MT provides important visual motion inputs that drive the initiation of pursuit, but not for steady-state tracking. Neurons in MT are selectively sensitive to moving stimuli and tuned for both the direction and speed of motion. Thus, we knew that we would find a representation of the model's image velocity pathway in MT. We recorded from MT in anesthetized monkeys so that we could study neurons for hours using an extensive set of target motions, without the confound of the monkey tracking the target and changing the visual stimulus.

We discovered correlates of the motion-onset and smooth-image-acceleration pathways, but we did not find the image deceleration signal

needed to prevent overshoot of eye velocity after the initiation of pursuit (Lisberger & Movshon, 1999). We used target motions that ramped from zero to a fixed speed and then back down to zero so that we could compare the responses of MT neurons to the same set of target speeds but during acceleration versus deceleration. Many neurons showed impressive differences in firing rate for acceleration versus deceleration (see Figure 1D), implying that image acceleration and deceleration might be represented in the MT population. Further, the transient firing of MT neurons at the onset of stimulus motion provided a clear correlate of the motion onset pathway in the image-motion model. In fact, different neurons showed different degrees of acceleration-deceleration asymmetry (ADA; see Figure 1E). We were able to capitalize on the diversity of acceleration-deceleration asymmetries to recover stimulus acceleration. We did so by weighting each neuron in the population by its ADA. A parallel computation recovered stimulus speed by weighting each neuron by its preferred speed (see Figure 1F). However, we were not able to recover image deceleration. Thus, our analysis of the signals emanating from MT did not seem to support fully the need of the image-motion model for a visual signal related to image deceleration, an issue that remains unresolved to this day.

3 Visual-Motor Gain

The next step in creating a model of pursuit came from the realization that one component of the system controls the strength, or gain, of the transmission of visual signals to the motor system. Others had suggested that pursuit needed to be turned on when a target moved based on the conclusions that fixation and pursuit probably are different subsystems and that fixation probably is not pursuit of zero target speed (Robinson, 1965; Luebke & Robinson, 1988). We codified the process of switching pursuit "on" experimentally and showed that the underlying process was a volume control, not a switch (Schwartz & Lisberger, 1994).

Our experiments provided a brief perturbation of target motion during steady-state pursuit tracking (see Figure 2D, black trace and arrow). We measured the eye velocity response to the perturbation alone (red trace and arrow) by subtracting the eye velocity trace for the same target motion without a perturbation. Then we compared the eye velocity response to the same perturbation delivered during steady-state pursuit versus during fixation (see Figure 2E). The response to the perturbation was much larger during pursuit than during fixation, even though the retinal image motion was nearly identical in the two conditions. Experiments not summarized here demonstrate that the gain of visual-motor transmission is speed tuned and directional. The size of the eye velocity response to the perturbation increases smoothly as a function of the ongoing pursuit eye speed and is larger for a perturbation along the axis of target motion versus orthogonal to the axis of target motion. Thus, visual motion signals have much higher

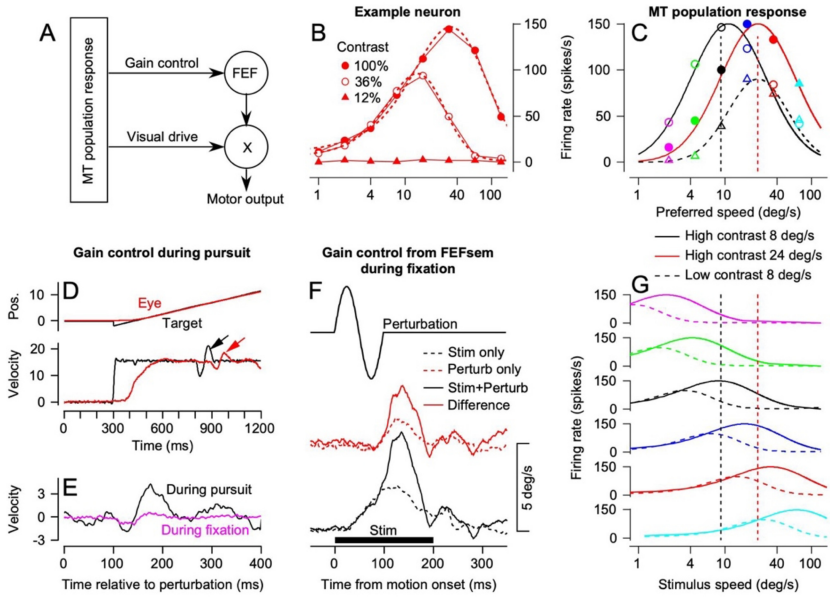

Figure 2: Evidence for control of the gain of visual-motor transmission, role of FEF_{SEM}, and effect of gain control on pursuit of low-contrast targets. (A) Two-pathway model of pursuit based on the existence of gain control. (B) Speed-tuning curves of an example MT neuron for targets with 100%, 36%, and 12% contrast. (C) Model MT population responses derived from curves in panel G. Open circles show model for high-contrast target motion at 8 deg/s, filled circuits show model for high-contrast target motion at 24 deg/s, and open triangles show model for low-contrast target motion at 8 deg/s. (D) Experimental paradigm to demonstrate gain control. Black arrow points to a brief perturbation of target motion during steady-state pursuit, and red arrow points to the eye velocity response. (E) Black and magenta traces compare responses to the same perturbation presented during steady-state pursuit and fixation of a stationary target. (F) Evidence that FEF_{SEM} controls the gain of visual-motor transmission. Top trace shows the perturbation presented during fixation. Traces are dashed black trace, response to microstimulation alone in FEF_{SEM}; dashed red trace, response to perturbation alone during fixation; continuous black trace, response to perturbation during microstimulation; solid red trace, response to perturbation during microstimulation. (G) Speed tuning curves for model MT neurons. Continuous and dashed traces show simulated responses for high- and low-contrast target motion. Figures are modified, with permission, from Egger and Lisberger (2022), Schwartz and Lisberger (1994), and Tanaka and Lisberger (2001). Panel B presents unpublished data from J. Yang and S. G. Lisberger.

gain access to the motor system during pursuit than during fixation and the gain of visual-motor transmission is adjustable smoothly (Schwartz & Lisberger, 1994).

The smooth eye movement region of the frontal eye fields (FEF_{SEM}) plays a major role in controlling the gain of visual-motor transmission. On a hunch, we introduced microelectrodes into FEF_{SEM} and performed microstimulation at sites where the neurons discharged vigorously in relation to smooth pursuit eye movements (Tanaka & Lisberger, 2001). At suprathreshold intensities, stimulation evokes a smooth eye movement. At much lower intensities, stimulation increases the size of the response to a perturbation of target motion during fixation, while evoking only a small smooth eye movement. Support for this assertion appears in Figure 2F.

Presentation of a perturbation of target motion during fixation causes a small smooth eye velocity (dashed red trace). Stimulation of FEF_{SEM} alone also causes a small smooth eye velocity (black dashed trace). Presentation of the same perturbation of target motion during stimulation of FEF_{SEM} causes a much larger eye movement (solid black trace). Subtraction of the eye movement induced by microstimulation alone from that induced by a perturbation during microstimulation leaves a response to the perturbation that is much larger during stimulation (solid red trace) than without stimulation (dashed red trace). Thus, the output from FEF_{SEM} controls the gain of visual-motor transmission.

The discovery of gain control led to the development of two-pathway models (see Figure 2A). Visual motion inputs arise in the responses of the population of neurons in MT. One pathway provides visual drive for pursuit and the other pathway, through FEF_{SEM}, sets the gain of visual-motor transmission. We will see later that the two-pathway configuration has two major virtues: it fits with the biology of two parallel pathways from MT to the motor system, and it allows the models to account for a lot of behavioral data based on visual inputs from realistic models of MT population responses.

3.1 Explanatory Power of Gain Control. The demonstration of gain control provides an answer for one paradox in the effects of stimulus contrast and target speed on the initiation of pursuit. It explains how the eye velocity at the initiation of pursuit can increase as a function of target speed yet decrease when the contrast of the visual stimulus is reduced. The paradox arises because of experimental observations on how the response of the population of MT neurons changes as a function of target speed and contrast, discussed below.

One theory of how pursuit estimates target speed from the population response in MT (Born, Groh, Zhao, & Lukasewycz, 2000; Groh, 2001; Churchland & Lisberger, 2001b; Priebe, Churchland, & Lisberger, 2001; Priebe & Lisberger, 2004) is based on the speed-tuned responses of MT neurons:

pursuit finds the preferred speed at the peak of the population response by computing the "vector average":

$$S = \frac{\sum_i R_i^{MT} S_i^{pref}}{\epsilon + \sum_i R_i^{MT}}. \tag{3.1}$$

Here, S is the estimate of target speed, and R_i^{MT} and S_i^{pref} are the response and preferred speed of the ith MT neuron. The constant ε confers noise immunity at low response amplitudes and renders the estimate of target speed S somewhat sensitive to the amplitude of the population response.

Vector averaging (i.e., equation 3.1) accounts for the effect of target speed on the initiation of pursuit (Gardner, Tokiyama, & Lisberger, 2004). To visualize the MT population response, we assemble the responses of all neurons in the population by plotting each neuron's response as a function of its preferred speed. In Figure 2C, for example, the open and filled circles show the responses of the population of six neurons for target speeds of 8 and 24 deg/s, taken from the solid speed tuning curves in Figure 2G by measuring firing rate at the vertical black and red dashed lines. Higher target speed creates a population response that peaks at higher values of preferred speed but retains the same amplitude. Vector averaging finds the preferred speed at the peak of the population response, and so it estimates the correct target speed, as does the initiation of pursuit.

Vector averaging needs gain control to account for the effect of target contrast on the initiation of pursuit. Lower-contrast targets produce lower speeds at the initiation of pursuit. Yet recordings from MT (Krekelberg, van Wezel, & Albright, 2006; J. Yang & S. G. Lisberger, unpublished data) indicate that the population response in MT shifts toward higher preferred speeds when target contrast is decreased (see Figure 2C, open triangles versus open circles), even though the amplitudes of the responses decrease for all neurons (see Figures 2B, 2C, and 2G). We account for the decrease in eye velocity in the initiation of pursuit with the suggestion that reduced contrast creates a less reliable visual motion signal in MT because it decreases the amplitude (and likely the signal-to-noise ratio) of the population response (Darlington, Tokiyama, & Lisberger, 2017). FEF_{SEM} interprets the less reliable motion signal as a caution that visual-motor gain should be low. Although vector averaging estimates a higher target speed for lower contrast targets, visual-motor gain counteracts that effect. As a result, the eye velocity at the initiation of pursuit decreases as a function of target contrast even as the population response in MT moves toward higher preferred speeds.

3.2 Control of Visual-Motor Gain by Motion Reliability. A merger of the models in Figures 1 and 2 cements the conceptual role of motion reliability and gain control in the pursuit system by reproducing the effect of changes in the coherence of a patch of moving dots on pursuit (Behling

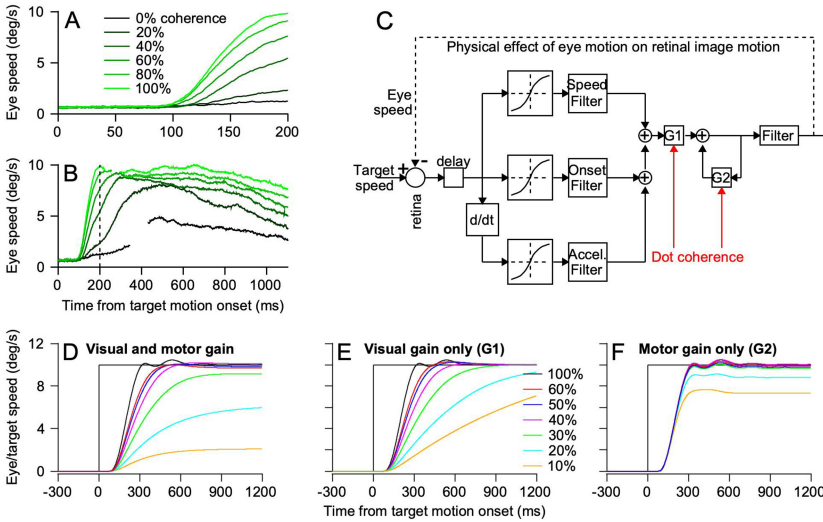

Figure 3: Gain control added to the image-motion model accounts for the effect of reduced dot coherence on the initiation and steady state of pursuit. (A, B) Fast and slow time-base records show the effect of coherence on the initiation of pursuit (A) and steady-state tracking (B). Different shades of green show data for different dot coherences. (C) Image motion model from Figure 1, modified to allow dot coherence to modulate both the gain of visual-motor transmission via G_1 and the gain of eye velocity positive feedback to support steady-state tracking via G_2. (D–F) Effect of dot coherence on the output of the model when modulating both visual and motor gain (D), visual gain only (E), and motor gain only (F). Different colors show model output for different simulated dot coherences. Figure assembled, with permission, from multiple figures in Behling and Lisberger (2020).

& Lisberger, 2020). Decreasing the coherence of motion within a patch of dots from 100% to 80%, 60%, 40%, 20%, and 0% causes decreases in the rate of eye acceleration at the initiation of pursuit (see Figure 3A). It also affects steady-state tracking by causing the system to settle at stable steady-state eye speeds well below target speed (see Figure 3B). Here, we note that the weak but nonzero pursuit of 0% coherence dots is probably due to the monkey's ability to weakly track the virtual aperture around the patch of dots even without a local motion signal. Other experiments show that the pursuit system still is responsive to pulses of target speed during poor steady-state tracking, implying that a nonvisual component of pursuit must account for the poor steady-state tracking.

We account for the effect of dot coherence on the initiation of pursuit in the model of Figure 3C by adding the gain element G_1 to the image

motion model from Figure 1B. G_1 is the instantiation in this model of the gain control provided by FEF_{SEM} in Figure 2A; the model places G_1 under the control of dot coherence (i.e., motion reliability).

We account for the effect of dot coherence on steady-state tracking by allowing it to control the value of G_2 in the model of Figure 3C. G_2 lies within a positive feedback pathway that uses a corollary discharge of eye velocity as part of the eye movement command and thereby sustains perfect tracking in the absence of image motion. Our simple models are based on neural recordings (Lisberger & Fuchs, 1978; Stone & Lisberger, 1990), showing that the floccular complex of the cerebellum is part of a positive feedback pathway that receives a corollary discharge of eye velocity from time $t - \Delta t$ and uses the corollary discharge to control eye velocity at time t. Thus, nonvisual signals control the quality of steady-state tracking and keep the eyes moving smoothly at target speed even in the absence of image motion; image motion causes changes in eye velocity to correct any tracking errors. Simulation of the model in Figure 3C shows that it reproduces both of the effects of reduced dot coherence only if we allow modulation of both G_1 and G_2 by dot coherence (see Figure 3D). Modulation of G_1 only (see Figure 3E) or G_2 only (see Figure 3F) fails to reproduce the biological data (Behling & Lisberger, 2020).

In biological terms, we understand the effect of reduced dot coherence as an effect on the internal reliability, or signal-to-noise, of the representation of motion in MT. We predict (and preliminary data confirm) that reduced dot coherence causes a reduction in the amplitude of the MT population response while keeping the preferred speed at the peak of the population response fixed at target speed (Stuart Behling & Stephen Lisberger, unpublished data). We predict that FEF_{SEM} produces lower output, and therefore a lower gain of visual-motor transmission, during pursuit initiation and steady state because the reliability of the motion signal is lower. We also predict (as yet untested) that the gain of the positive feedback of eye velocity through the cerebellar floccular complex is reduced by lower dot coherences.

4 Models Reimagined Based on Single-Trial Data

In the early part of this century, our approach to understanding and modeling the pursuit circuit was transformed by our realization of the explanatory power of trial-by-trial analysis of behavior and neural responses. This occurred after three decades of thinking in terms of "lumped" models that reproduced averaged behavioral data (e.g., as in Figures 1B and 3C), and it changed how we do our experiments as well as how we think.

The initiation of pursuit varies from trial-to-trial in an interesting and revealing way (Osborne, Lisberger, & Bialek, 2005). The traces from 17 single trials in Figure 4C show the magnitude of the trial-by-trial variation in eye speed and emphasize that the magnitude of variation far exceeds the

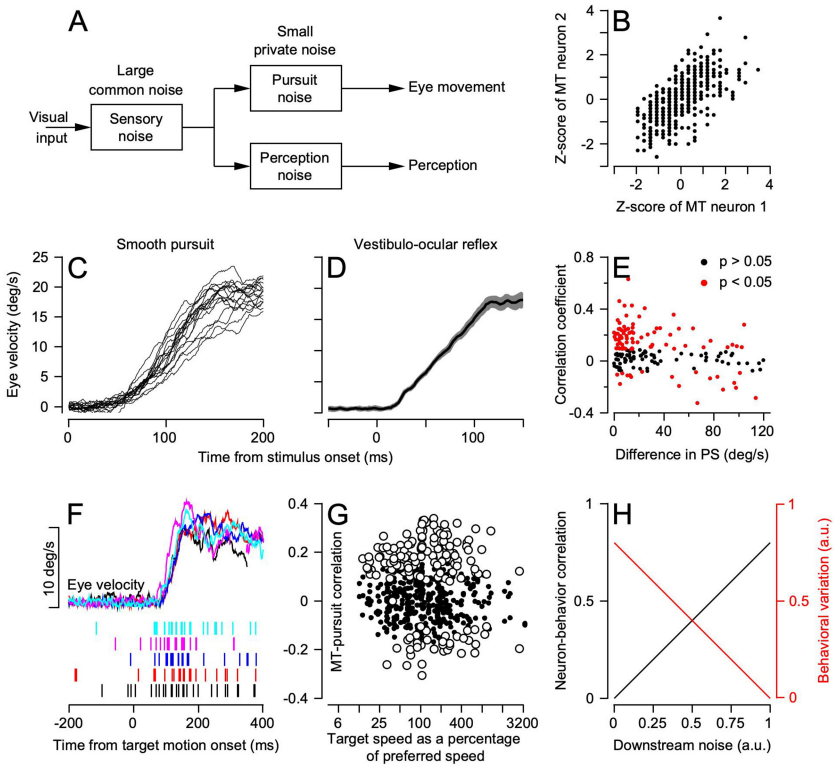

Figure 4: Analysis of trial-by-trial variation in pursuit eye velocity and responses in area MT. (A) Conceptual model of sources of trial-by-trial variation in pursuit and perception. (B) Trial-by-trial correlation of z-scored responses of two MT neurons with a strong noise correlation. (C) Trial-by-trial variation in 17 single-trial examples of the initiation of pursuit. (D) Much smaller trial-by-trial variation shown by the mean and standard deviation of eye velocity during the VOR. (E) Each symbol shows data for a different pair of MT neurons with neuron-neuron noise correlation plotted as a function of the difference between the preferred speeds of the two neurons. (F) Example traces and single trial rasters showing data used to compute MT-pursuit correlations. (G) Each symbol shows MT-pursuit correlation for a single neuron as a function of the target speed relative to preferred speed. Individual neurons appear multiple times for different target speeds. (H) Cartoon graph to illustrate the opposite effects of noise added downstream on behavioral variance and neuron-behavior correlation. Panels are replotted with permission from Lisberger (2010), Huang and Lisberger (2009), and Hohl et al. (2013).

variation in the vestibulo-ocular reflex (see Figure 4D) and therefore cannot be attributed to "motor noise." The single-trial traces of pursuit initiation also suggest that the variation in pursuit initiation is low dimensional: traces that start with lower eye speeds retain those lower eye speeds throughout the initiation of pursuit. We conclude that the variation is not just noise. Indeed, more than 90% of the variation of pursuit initiation can be accounted for in three dimensions: errors in estimating target speed, target direction, and the time of onset of target motion. Thus, it makes sense to think that the variation in pursuit initiation originates from the sensory representation of visual motion and not from motor processing. Indeed, the limits on precision in pursuit and visual motion perception are similar, leading to the conceptual model of Figure 4A. Here, most of the variation in pursuit and perception has a shared origin in the sensory system, and there are small, separate, private sources of variation.

Models designed to reproduce behavior data have limited power of explanation for how neural circuits generate sensory-motor behavior. To understand the origins of variation in pursuit initiation, we therefore turned to analysis of variation in neural responses. Our first finding, which does not yet appear in a neural circuit model, was a surprisingly large trial-by-trial correlation (neuron-behavior correlation) between the firing rate of Purkinje cells in the floccular complex of the cerebellum and the eye speed in the initiation of pursuit (Medina & Lisberger, 2007). In some Purkinje cells, the correlation coefficient was as high as 0.9, meaning that we could predict almost all of the variation in eye speed from the best correlated Purkinje cells. The average correlation was greater than 0.6.

It seems inescapable that the actual influence of each individual Purkinje cell on motor output is much smaller than suggested by the neuron-behavior correlations. Floccular Purkinje cells have disynaptic connections to motoneurons, but we estimate that more than 1000 Purkinje cells participate in each of horizontal and vertical pursuit. Instead, we attribute the remarkably high neuron-behavior correlations to coordination across the population of Purkinje cells. In the few pairs we were able to record, we confirmed neuron-neuron correlations between Purkinje cells that could account for the neuron-behavior correlations. This led to the understanding that high neuron-behavior correlations do not reveal the strength of influence of a given neuron on the behavior. Rather, they indicate correlation within a population of neurons that are collectively driving the behavior. Indeed, a neuron could show a large neuron-behavior correlation entirely through correlations with other neurons, without having any physical connection, itself, to the motor pathways for the behavior (Chaisanguanthum, Joshua, Medina, Bialek, & Lisberger, 2014).

Correlated variation in MT seems to be an important cause of trial-by-trial variation in the initiation of pursuit. The evidence for this statement is that neurons in MT have neuron-neuron noise correlations (Bair, Zohary, & Newsome, 2001; Huang & Lisberger, 2009) and neuron-behavior

correlations (Hohl, Chaisanguanthum, & Lisberger, 2013) during the initiation of pursuit ("MT-pursuit correlations"). In Figure 4B, for example, the symbols show data from multiple single trials for recordings from a pair of MT neurons. The graph plots the *z*-scored firing rate of one neuron versus another, revealing one example of impressive neuron-neuron noise correlations. Across the population of MT neurons, statistically significant neuron-neuron correlations occur in many pairs (see Figure 4E, red symbols) and correlations are larger for pairs of neurons with similar preferred speeds. The existence of neuron-neuron noise correlations does not alone mean that correlated sensory noise is a major cause of behavioral variation. The finding of MT-pursuit correlations does. We revealed MT-pursuit correlations by recording spikes in MT neurons and the simultaneous initiation of pursuit for up to 500 repetitions of the same visual stimulus (see Figure 4F). Many MT neurons had statistically significant MT-pursuit correlations that ranged as high as 0.4 and averaged 0.2 (see Figure 4G, open circles).

Computational modeling showed that the neuron-neuron correlations in MT could create both the MT-pursuit correlations and the variation in pursuit (Huang & Lisberger, 2009; Hohl et al., 2013). Further, the presence of large MT-pursuit correlations argues strongly that much of the behavioral variation arises from the sensory representation. Noise is possible downstream, of course, but it has conflicting effects on MT-pursuit correlations and behavioral variation (Schoppik, Nagel, & Lisberger, 2008; Egger & Lisberger, 2022). If noise is added downstream, then behavioral variance will increase relative to what would be caused by a given amplitude and structure of neuron-neuron correlations in MT (see Figure 4H, black line). At the same time, noise added downstream will create behavioral variance that cannot be attributed to correlated noise in MT and would decrease MT-pursuit correlations (see Figure 4H, red line). As we will see, there could be an exact balance of correlated noise in MT and downstream noise that will reproduce our data on both behavioral variation and MT-pursuit correlations.

5 A Model Sensory Decoder for Motor Control

We can think of the pursuit system as a decoder that transforms a sensory representation of visual motion into neural commands for movement. But I want to dispel our earlier notion that we can think of the decoder as a simple equation such as vector averaging (see equation 3.1). Instead, we should think of the entire circuit downstream from MT as a complex neural decoder that comprises at least two major pathways with different functions (see Figures 2A and 5A). *One pathway* estimates the parameters of motion. We think of this pathway in terms of direct projections from area MT and its motion companion area MST to brainstem nuclei: the dorsolateral pontine nucleus (DLPN) and the nucleus reticularis tegmenti pontis (NRTP). The *other pathway* uses multiple inputs, including from MT, to create a gain

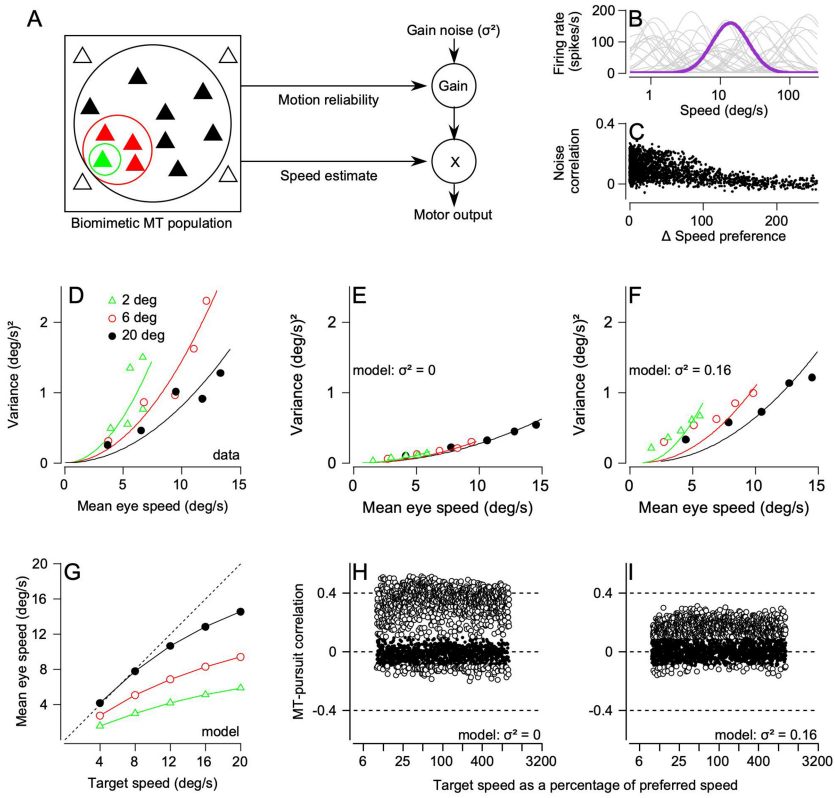

Figure 5: A biomimetic computational model that accounts for first- and second-order statistics of behavioral and MT neural responses. (A) Schematic of the model; equations available in Egger and Lisberger (2022). (B) Diversity of amplitude and preferred speeds in tuning curves of model MT neurons. (C) Noise correlation among pairs of model MT neurons as a function of the difference in preferred speed of the two neurons. (D) Data showing variance of eye speed at the initiation of pursuit as a function of mean eye speed for targets comprising 2, 6, and 20 deg patches of dots. (E, F) Model predictions for variance of eye speed as a function of mean eye speed for different size targets, with values of 0 (E) or 0.16 (F) for noise in the gain control pathway. (G) Model predictions of eye speed as a function of target speed for three target sizes. (H, I) Model predictions for MT-pursuit correlation as a function of the relationship between target speed and preferred speed with values of 0 (H) or 0.16 (I) for noise in the gain control pathway. Data reproduced with permission from Egger and Lisberger (2022).

signal that is based on motion reliability, expectations based on past experience, and other factors. The broader vision of a decoder reframes the challenge of understanding how motion signals are decoded to create commands for pursuit. The challenge is expanded to comprise determining the organization and operation of the multiple parallel neural circuits from MT to the final motor pathways. These circuits are the sensory decoder for pursuit motor control, and they probably cannot be characterized by any simple equation.

We made the next step toward a more biologically motivated model of the sensory decoder for pursuit based on a simple observation about the relationship between the variance and mean of eye velocity in the initiation of pursuit (Egger & Lisberger, 2022). Increasing the size of a tracking stimulus from 2 to 6 to 20 degree breaks the traditional relationship (Harris & Wolpert, 1998) between the variance and mean of motor output (see Figure 5D). "Signal dependent noise" no longer holds, meaning at least that the source of noise cannot be in the final motor pathways and instead must be in the sensory representations and the sensory decoder for motor control.

We reproduced a large body of data with a model (Egger & Lisberger, 2022) where the sensory decoder explicitly includes two pathways (see Figure 5A). In the decoder, noise arises from both a correlated variation in the MT population response, as before, and in the gain control pathway. With reasonable assumptions, the model was able to reproduce accurately the magnitude of variation in the initiation of pursuit, the effects of increasing the size of the pursuit stimulus on the mean and variance of eye velocity at the initiation of pursuit, and the observed trial-by-trial variation in MT responses. We included model MT neurons with a wide range of tuning properties (see Figure 5B), appropriate neuron-neuron correlations (see Figure 5C), and realistic effects of increasing the size of the moving stimulus (Born & Tootell, 1992; Pack, Hunter, & Born, 2005). The equation for estimating motion reliability comprised a vector sum of the MT population response with each neuron's response weighted by the log of its preferred speed. The equation for estimating target speed comprised a vector average that depended somewhat on the amplitude of the population response, as in equation 3.1. The model does an excellent job of reproducing the mean eye velocity at the initiation of pursuit as a function of target size and speed (see Figure 5G).

If the gain control pathway is endowed with noise that is independent of the correlated variation in MT responses, then the model reproduces both the effect of target size on the variance of eye speed (see Figure 5F) and the amplitude and distribution of MT-pursuit correlations (see Figure 5I). If the gain control is noiseless, the model predicts a variance of eye speed that is unrealistically low and does not depend on target size (see Figure 5E). The model with noiseless gain control also predicts MT-pursuit correlations (see Figure 5H) that are considerably larger than those recorded in

the monkey (see Figure 4G). Thus, the two-component sensory decoder has considerable predictive value. In addition, it makes the testable prediction of strong trial-by-trial correlations between the activity of FEF_{SEM} neurons and the eye speed at pursuit initiation (Schoppik et al., 2008), but without correlations between the activity of neurons in FEF_{SEM} and MT.

6 A Neural Circuit Basis for Bayesian-Like Behavior in Motor Control

The initiation of pursuit is based on a reliability-weighted combination of sensory data from the visual motion system and priors based on past experience (Yang, Lee, & Lisberger, 2012; Orban de Xivry et al., 2013; Darlington et al., 2017). To demonstrate this feature of pursuit and study its neural basis, we presented different blends of target speeds in blocks that were designed to control the pursuit system's expectations of target speed (see Figure 6A). In the "fast context," 80% of targets moved at 20 deg/s and 20% moved at 10 deg/s. In the "slow context," 80% of targets moved at 2 deg/s and 20% moved at 10 deg/s. The 10 deg/s target motions were part of both contexts and therefore served as a probe for the effects of having either fast or slow target motions in most of the trials. We used high- and low-contrast targets to control the reliability of visual motion signals. Under these conditions, target speed context had a modest effect on the initiation of pursuit for 10 deg/s motion of high-contrast targets and a considerably larger effect for 10 deg/s motion of low-contrast targets (see Figure 6B, green versus blue histograms).

A larger effect of context for sensory data of lower reliability is exactly what is expected of a system the shows Bayesian-like behavior. Further, computational modeling shows that it is possible to understand the implementation of Bayesian-like behavior in terms of control of sensory-motor gain (Darlington et al., 2017). Expectations of a faster target speed should increase the firing of neurons in FEF_{SEM} and lead to a higher gain of visual-motor transmission. Lower-contrast targets should cause lower firing in FEF_{SEM} and lead to a lower gain of visual-motor transmission.

Recordings from FEF_{SEM} reveal all the components of the reliability-weighted combination of priors and sensory data and support the idea that gain control plays an important role in the associated pursuit behavior (Darlington, Beck, & Lisberger, 2018). During recordings, we placed the monkey alternately in 50-trial blocks of fast- or slow-context trials. In each trial, the monkey fixated for 800 to 1600 ms before he had to pursue a moving target. During the fixation interval, we saw a neural correlate of a prior based in expectations. Firing rate ramped up in preparation for the onset of target motion and reached a level that was higher in the fast context compared to the slow context. This finding appears in traces in Figure 6D that are aligned so that they end at the termination of fixation and the start of target motion. During the initiation of pursuit (see Figure 6E), neurons in FEF_{SEM} show evidence of the same combination of priors and sensory data as does pursuit

behavior. Here, the traces start at the end of fixation and the start of target motion. For high-contrast targets, the response is essentially the same in both the fast and slow contexts (green versus blue continuous traces). For low-contrast targets, the response to low-contrast targets is both delayed and reduced in amplitude relative to that for high-contrast targets. Thus, the output of FEF_{SEM} during pursuit initiation is appropriate to control the gain of visual-motor transmission in a way that implements Bayesian behavior. The gain signal depends weakly on the prior when the sensory data come from high-contrast targets and are highly reliable; it depends more strongly on the prior when the sensory data come from low-contrast targets and are less reliable.

A simple neural network with fully recurrent connections among excitatory and inhibitory model neurons (see Figure 6C) reproduces all the features of our recordings from FEF_{SEM}. The network receives two inputs: a pulse of activity from visual motion processing with an amplitude that depends on stimulus contrast and a step of activity to indicate the time of fixation. The average response of the model units (see Figure 6G) shows preparatory activity that increases steadily during fixation. When the context changes from control to slow to fast and back to control, the preparatory activity in the model follows the same trajectory as the data (Figure 6H) because of plasticity placed strategically at the recurrent synapses from excitatory neurons. Thus, preparatory activity learns based on experience and reaches a peak at the time of motion onset (see Figure 6G, vertical arrow) that is larger in the fast versus slow context. After motion onset, the model neurons show a pulse of firing that is larger for high- versus low-contrast targets (continuous versus dashed traces) and reaches a higher peak firing in the fast- versus slow-context (red versus black traces). As in the data (see Figure 6K), the size of the pursuit-related pulse of activity in the model (see Figure 6L) is related to and larger than the modulation associated with the preparatory activity.

One theme of our research in the past few years is the value of trial-by-trial analyses in constraining and guiding efforts to create a computational model of pursuit. In this regard, it is important that the network model of FEF_{SEM} uses shunting inhibition to create the same trial-by-trial correlations between preparatory and pursuit-related activity as do the data (Darlington et al., 2018). Our analyses defined three different measures of the pursuit-related pulses of firing rate (see Figure 6F): the absolute modulation of firing rate ("absolute"), the preparatory modulation of firing rate ("prep"), and the incremental modulation from preparatory to the peak ("incremental"). Analysis of single-trial firing rates for FEF_{SEM} neurons showed that the absolute modulation of firing rate was correlated positively with the preparatory activity (see Figures 6I and M). In contrast, the incremental change in firing was correlated negatively with the preparatory activity (see Figure 6N). All model neurons in the successful network showed the same trial-by-trial effects (see Figure 6J). Thus, a generic cortical neural circuit model

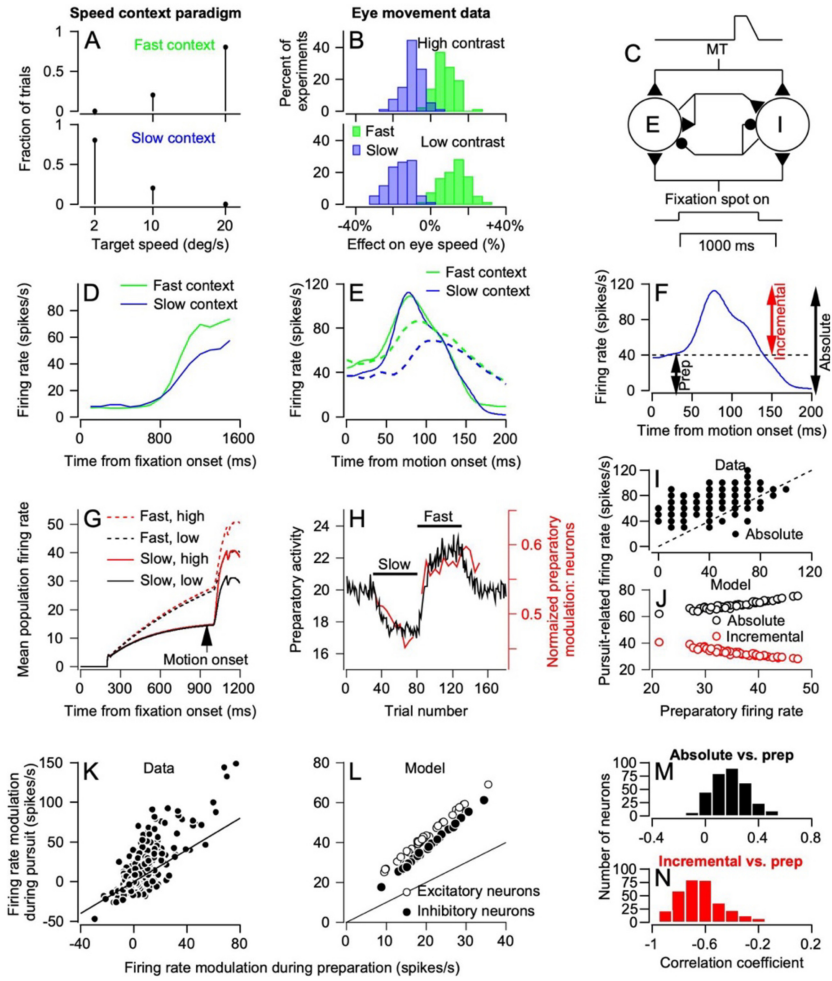

Figure 6: Representation of all components of Bayesian-like behavior in responses of neurons in FEF_{SEM}. (A) Schematic showing the blend of target speeds in "fast" and "slow" contexts. (B) Evidence of reliability-weighted combination of sensory data and expectations based on previous experience in the initiation of pursuit. (C) Schematic of neural network model used to simulate responses in FEF_{SEM}. (D) Preparatory activity in data from FEF_{SEM} neurons and the effect of target speed context on its amplitude, aligned on the end of fixation at $t =$ 1600 ms. (E) Pursuit-related activity in data from FEF_{SEM} neurons and the effect of target speed context and target contrast, aligned on the onset of target motion. (F) Schematic showing the different measures we used of FEF_{SEM} activity to obtain the plots in panels I, J, M, and N. (G) Prediction of preparatory and pursuit-related activity by the model circuit and the effect of target speed context and target contrast. (H) Time course of adaptation of amplitude of preparatory

can, with a few strategic additions of plasticity and shunting inhibition, reproduce the activity of neurons that represent all of the components of Bayesian-like behavior.

Importantly, we do not think of the network in Figure 6C as a "Bayesian" circuit, nor do we think that it is particularly significant that the pursuit system can be seen as having Bayesian-like behavior. Rather, we see the terminology of "Bayesian" as a metaphor for a reliability-weighted combination of sensory data with adaptable expectations based on experience. We conclude that the existence of a gain-control mechanism in pursuit allows the FEF_{SEM} to play a key role in (1) regulating the pursuit response under different conditions of expectations and movement preparation, (2) assessing the reliability of the motion signals for pursuit, and (3) allowing the system to combine sensory data with expectations in an optimal manner.

7 Next Steps: An Aspirational Model

Over the past 40 years, our approach to modeling the pursuit system has evolved to become more oriented toward biologically motivated or biomimetic models. We have moved from control theory models that aimed only to account for average pursuit behavior, to models that are based on biologically motivated model MT population responses, to models that recognize the complicated, parallel, multicomponent organization of the sensory-motor decoder. We have moved from models that reproduce average responses, to models that reproduce single trial responses, to models that are constrained by trial-by-trial neuron-neuron and neuron-behavior correlations. This is progress, but I would say that we have taken baby steps rather than large, bold strides.

To conclude this review, I evaluate the requirements for a biomimetic model, trying to be forthright about where we are, to outline where we need to be, and to offer a strategy for getting there.

1. The model needs to include all nodes of the biological pursuit circuit and the connections among them (see Figure 7). The areas that we understand well enough to include in the model right now are MT (and its visual

activity in switches between fast and slow speed contexts. Black trace shows the prediction of the model; red trace shows normalized data. (I, J) Trial-by-trial correlations of pursuit-related versus preparatory firing rate for data (I) and model neurons (J) for different measures of responses. Each symbol plots data from one real or simulated trial. (K, L) Firing rate modulation during pursuit initiation versus that during preparation for data (K) and model L. (M, N) Distribution across data from neurons of trial-by-trial correlations between pursuit and preparatory firing rate for absolute (M) versus incremental (N) firing rate. All panels reproduced with permission from Darlington et al. (2018).

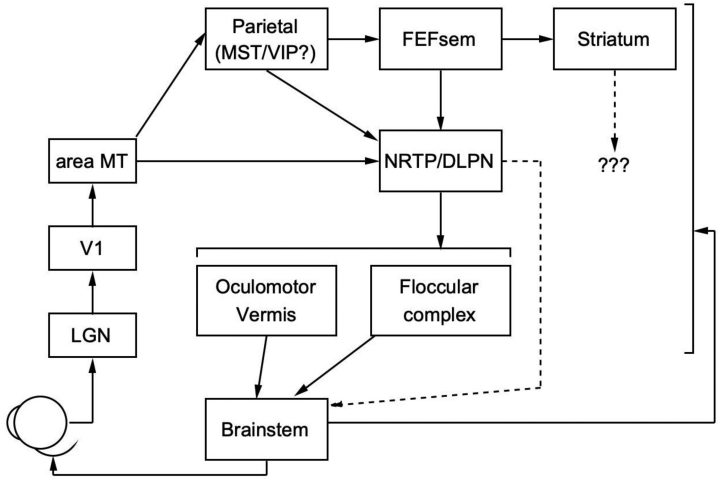

Figure 7: A schematic diagram of the anatomical connections within the pursuit system.

inputs from V1/LGN), FEF_{SEM}, and the floccular complex of the cerebellum. My lab has recorded good samples of neurons in the DLPN and NRTP; preliminary analysis indicates that important transformations occur between the cerebral cortex and these traditional "relay" nuclei. Nevertheless, considerable processing must still occur downstream (Darlington & Lisberger, 2022). For other areas, their anatomical access to the pursuit circuit is unknown. We know that the oculomotor vermis projects to the fastigial nucleus and plays an important role in pursuit (Kase, Noda, Suzuki, & Miller, 1979; Dash, Catz, Dicke, & Thier, 2012; Kurkin et al., 2014), but we are challenged to interpret neural responses in the oculomotor vermis because we lack knowledge of the anatomical or functional connection from the fastigial nucleus to the final motor pathways. We know that neurons in the striatum respond during pursuit (Basso, Pokorny, & Liu, 2005), but without knowledge of how those signals access the final motor pathways. We know very little about the site or properties of neurons in the parietal cortex that are part of the cortico-cortical pathways from MT to FEF_{SEM} (Dursteler & Wurtz, 1988; Churchland & Lisberger, 2005). Perhaps most important, we have essentially zero information about cell type. Given the inexorable diversity in response profiles across the population of neurons recorded in each area, we must be able to identify projection neurons versus local interneurons. We need to classify excitatory versus inhibitory neurons while recording from the brain of an awake, behaving primate. This essential clue to system function awaits more systematic deployment of modern molecular cell-typing methods in nonhuman primates.

2. The model needs to reproduce neural responses and behavioral data across a wide range of behavioral paradigms. Questions that need to be answered include at least the direction and speed tuning properties at different nodes of the circuit, the impact of stimulus form (especially motion reliability), and the presence or absence of preparatory activity (Darlington et al., 2018; Darlington & Lisberger, 2020, 2022). It also would be helpful to use brief pulses of target motion under different conditions to assess whether and how a given neuron participates in the neural mechanisms that control the gain of visual-motor transmission. Does each specific neuron sit before gain control, after gain control, or as part of gain control? Again, we have published sufficient data from MT and FEF_{SEM}, and we have preliminary data from NRTP and DLPN. But we do not know whether Purkinje cells in the floccular complex show the preparatory activity we see elsewhere in the system, or whether their responses scale as expected with eye velocity under different conditions of visual-motor gain. Modern recording technology with multicontact probes affords better stability than previous approaches with single electrodes, as well as faster accumulation of neural populations. We need to return to areas such as the floccular complex, the basal ganglia, and the oculomotor vermis to understand their responses across a wide range of behavioral and stimulus conditions, preferably with some degree of cell-type classification.

3. The model needs to include local circuits that perform local computations, as well as recurrent connections that deliver corollary discharge signals from the motor pathways back to the cerebral cortex and basal ganglia. In the past, we have focused on the macro-organization of the feedforward pursuit circuit with a skeleton diagram like Figure 7. One of the lessons from our neural network model of FEF_{SEM} (Darlington et al., 2018) is that important computations are performed by microcircuits within nodes of the circuit. Perhaps the diversity of response profiles within each node provides a clue to the computations performed within each node; perhaps identifying unique response properties in projection neurons will reveal which neurons are local interneurons and unlock the analysis of those local computations. A second lesson from FEF_{SEM} is the need to consider recurrent feedback of corollary discharge from the motor pathways. Many neurons in FEF_{SEM} discharge a pulse of activity during pursuit initiation and show sustained activity during steady-state tracking (Tanaka & Lisberger, 2002). Where does the sustained activity come from? Is it generated autonomously in FEF_{SEM}, or does it originate in recurrent feedback from the motor system such as we have demonstrated in the floccular complex of the cerebellum? The same question exists for other nodes, including the oculomotor vermis, basal ganglia, NRTP, and DLPN.

4. The model needs to operate in negative feedback configuration where the act of tracking alters the image motion input to the system and largely eliminates image motion during steady-state tracking. The model needs to

account for eye velocity and neural firing rate as a function of time. Ours and others' initial control theory models included time and dynamics and operated in feedback configuration, but this got lost as we attempted to transition to models that had more biologically realistic internals. The early models identified a number of features that are challenging to explain—for example, absence of overshoot at the initiation of pursuit (Krauzlis & Lisberger, 1989); spontaneous oscillations at higher frequencies than predicted purely by image velocity inputs (Goldreich et al., 1992); and essentially perfect steady-state tracking, eliminating the image motion drive to the system (Morris & Lisberger, 1987). Our first attempt to replace the control theory representation of visual motion signals with a realistic MT population response that varied as a function of time was only partially successful (Lisberger & Movshon, 1999). Instead, our recent, more "biologically realistic" models have represented neural responses as static spike counts rather than as time-varying firing rates or spike trains. We need to return to models with feedback and temporal dynamics.

5. The model needs to have realistic trial-by-trial variation, neuron-neuron correlations, and neuron-behavior correlations. We started 40 years ago with the idea that we needed to reproduce average data. More recent efforts (e.g., Figure 5) show the value of the single-trial data and simultaneous recordings from multiple neurons as constraints on models. Especially powerful are constraints that play off against each other, as do the variance of pursuit initiation and the amplitude of MT-pursuit correlations. I think that trial-by-trial data from other areas, including analysis as a function of time, hold promise for constraining future, more biologically realistic models.

Given the need for new data from more nodes of the pursuit circuit using a broader set of behavioral paradigms and stimulus speeds and forms, it would be reasonable to ask whether data collection should precede further development of a biomimetic computational model of the pursuit circuit. I think not. I think that it would be constructive to create a computational model of pursuit now, even given fragmentary data.

I suggest the model in Figure 8 as a starting point that can guide experiments and make testable predictions. It is an open-loop model that accounts for the initiation of pursuit and steady-state tracking based on the responses of a biomimetic model population of MT neurons across the full pursuit response (colored traces at center of figure), complete with realistic neuron-neuron correlations. The output from MT goes (1) directly to DLPN and NRTP in the pons and (2) into a neural circuit model that reproduces the responses of FEF_{SEM} neurons to the stimulus conditions in Figure 6. NRTP and DLPN, like FEF_{SEM}, contain local circuits that transform their inputs from MT and FEF_{SEM} and send outputs to the floccular complex of the cerebellum and maybe to the brainstem oculomotor areas. The next step would

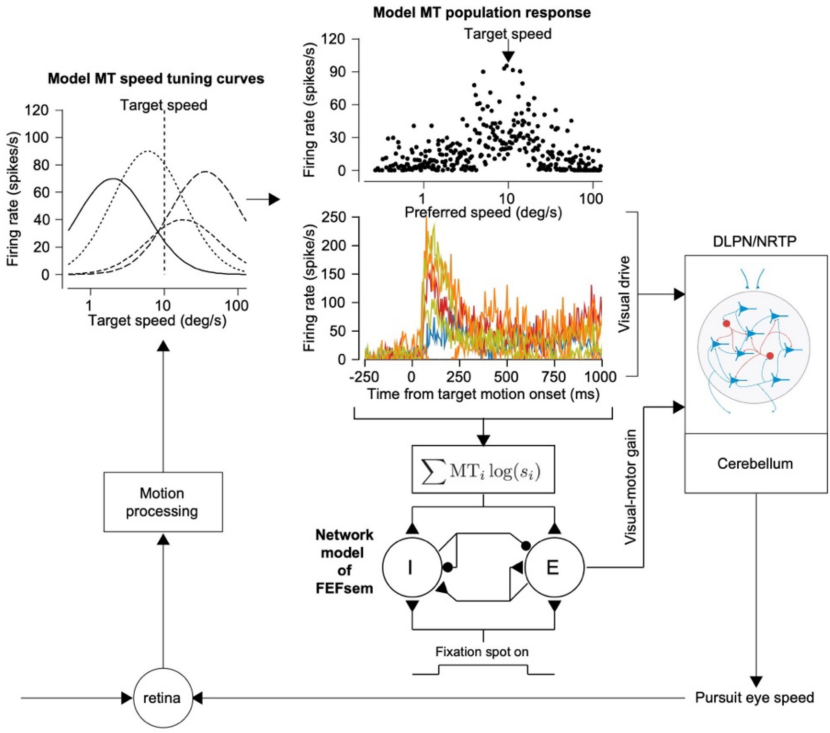

Figure 8: An aspirational model. The model (1) is dynamic, (2) is based largely on computations by model neural circuits rather than decoding equations, and (3) closes the feedback loop so that the sensory responses in MT are determined on the fly.

be to reconfigure the model so that its output feeds back and alters the retinal image motion inputs to the model, a feature that will require a dynamic model of the responses of MT neurons. The model in Figure 8 is incomplete, but it provides a vehicle for assembling a large amount of existing data and for motivating future experiments to further elaborate the details of the full pursuit circuit. It will be meaningful for how it explains what it can explain, and for what it cannot explain.

Finally, I ask whether the behavioral system and animal model I have chosen for study holds the correct promise for achieving a biomimetic circuit model of a sensory-motor behavior. In the 1970s and 1980s, we believed that recordings from single neurons in awake, behaving monkeys held the key to understanding how the brain works. In the 1990s, in the spirit of *Neural Computation*, we added computational modeling to our tool kit. Now

we have optogenetics, calcium imaging, and multicontact recording probes that are deployed most easily and very commonly in mice.

I see a gap here. It is a challenge to apply modern technologies in nonhuman primates, and at least for some years, there is going to be a shortfall in the cell specificity of recording and stimulation. At the same time, I think there is great virtue in the strategy of adopting a highly quantifiable and controllable behavior and studying in quantitative detail the first- and second-order statistics of the relationships between neural responses and behavior. I do not see this happening in mice, at least not yet with the level of behavioral precision and granularity that is possible in the eye movement or arm movement system of nonhuman primates. In due course, NeuroPixel probes will be a game changer for analysis of circuit function in primates. They will allow simultaneous recordings of many neurons on potentially dozens of probes across multiple nodes of a single circuit. The resulting careful observations of the neural engine in action, in conjunction with quantitative analysis of well-understood behaviors, is arguably our most potent asset when trying to understand interesting neural computations. The interpretational power of neuron recordings in the eye movement system of monkeys is huge because we know how the discharge of neurons in many sites in the brain affects the activity of motoneurons to specific muscles. In the long run, I see a combination of modern technologies, quantitative analysis of behavior, recordings from multiple single neurons simultaneously in nonhuman primates, along with computational modeling with biomimetic neural circuit models, as an essential, critical component of neuroscience research.

Acknowledgments

I am grateful to many collaborators, graduate students, postdoctoral fellows, and technical staff for their contribution to my research program. I also thank the funding agencies that have supported the research, including the National Institutes of Health, the McKnight Foundation, and the Sloan Foundation. Current support is from NIH grant R01-EY027373.

References

Bair, W., Zohary, E., & Newsome, W. T. (2001). Correlated firing in macaque visual area MT: Time scales and relationship to behavior. *J. Neurosci.*, *21*, 1676–1697. 10.1523/JNEUROSCI.21-05-01676.2001, PubMed: 11222658

Basso, M. A., Pokorny, J. J., & Liu, P. (2005). Activity of substantia nigra pars reticulata neurons during smooth pursuit eye movements in monkeys. *Eur. J. Neurosci.*, *22*, 448–464. 10.1111/j.1460-9568.2005.04215.x, PubMed: 16045498

Behling, S., & Lisberger, S. G. (2020). Different mechanisms for modulation of the initiation and steady-state of smooth pursuit eye movements. *J. Neurophysiol.*, *123*, 1265–1276. 10.1152/jn.00710.2019, PubMed: 32073944

Born, R. T., Groh, J. M., Zhao, R., & Lukasewycz, S. J. (2000). Segregation of object and background motion in visual area MT: Effects of microstimulation on eye movements. *Neuron*, *26*, 725–734. 10.1016/S0896-6273(00)81208-8, PubMed: 10896167

Born, R. T., & Tootell, R. B. (1992). Segregation of global and local motion processing in primate middle temporal visual area. *Nature*, *357*, 497–499. 10.1038/357497a0, PubMed: 1608448

Chaisanguanthum, K. S, Joshua, M., Medina, J. F., Bialek, W. B., & Lisberger, S. G. (2014). The neural code for motor control in the cerebellum and oculomotor brainstem. *eNeuro*, *1*(1). 10.1523/ENEURO.0004-14.2014, PubMed: 26464956

Churchland, M., & Lisberger, S. G. (2001a). Experimental and computational analysis of monkey smooth pursuit eye movements. *J. Neurophysiol.*, *86*, 741–759. 10.1152/jn.2001.86.2.741

Churchland, M. M., & Lisberger, S. G. (2001b). Shifts in the population response in the middle temporal visual area parallel perceptual and motor illusions produced by apparent motion. *J. Neurosci.*, *21*, 9387–9402. 10.1523/JNEUROSCI.21-23-09387.2001

Churchland, K., & Lisberger, S. G. (2005). Discharge properties of MST neurons that project to the frontal pursuit area in macaque monkeys. *J. Neurophysiol.*, *94*, 1084–1090. 10.1152/jn.00196.2005, PubMed: 15872067

Darlington, T. R., Beck, J. M., & Lisberger, S. G. (2018). Neural implementation of Bayesian inference in a sensory-motor behavior. *Nat. Neurosci.*, *21*, 1442–1451. 10.1038/s41593-018-0233-y, PubMed: 30224803

Darlington T. R., & Lisberger, S. G. (2020). Mechanisms that allow cortical preparatory activity without inappropriate movement. *eLife*, *9*, e50962. 10.7554/eLife.50962, PubMed: 32081130

Darlington, T. R., & Lisberger, S. G. (2022). *Sensory-motor computations in a cortico-pontine pathway*. bioRxiv: 10.1101/2022.02.22.481514

Darlington, T. R., Tokiyama, S., & Lisberger, S. G. (2017). Control of the strength of visual-motor transmission as the mechanism of rapid adaptation of priors for Bayesian inference in smooth pursuit eye movements. *J. Neurophysiol.*, *118*, 1173–1189. 10.1152/jn.00282.2017, PubMed: 28592689

Dash, S., Catz, N., Dicke, P. W., & Thier, P. (2012). Encoding of smooth-pursuit eye movement initiation by a population of vermal Purkinje cells. *Cereb. Cortex*, *22*, 877–891. 10.1093/cercor/bhr153, PubMed: 21725035

Dursteler, M. R., & Wurtz, R. H. 1988. Pursuit and optokinetic deficits following lesions of cortical areas MT and MST. *J. Neurophysiol.*, *60*, 940–965. 10.1152/jn.1988.60.3.940, PubMed: 3171667

Egger S. W., & Lisberger, S. G. (2022). Neural structure of a sensory decoder for motor control. *Nature Comm.*, *13*, 1829. 10.1038/s41467-022-29457-4

Fuchs, A. F. (1967). Periodic eye tracking in the monkey. *J. Physiol.*, *193*, 161–171. 10.1113/jphysiol.1967.sp008349, PubMed: 16992282

Gardner, J. L., Tokiyama, S., & Lisberger, S. G. (2004). A population decoding framework for motion aftereffects on smooth pursuit eye movements. *J. Neurosci.*, *24*, 9035-9048. 10.1523/JNEUROSCI.0337-04.2004, PubMed: 15483122

Goldreich, D., Krauzlis, R. J., & Lisberger, S. G. (1992). Effect of changing feedback delay on spontaneous oscillations in smooth pursuit eye movements of monkeys. *J. Neurophysiol.*, *67*, 625–638. 10.1152/jn.1992.67.3.625, PubMed: 1578248

Groh, J. M. (2001). Converting neural signals from place codes to rate codes. *Biol. Cybern.*, *85*, 159–165. 10.1007/s004220100249, PubMed: 11561817

Harris, C. M., & Wolpert, D. M. (1998). Signal-dependent noise determines motor planning. *Nature*, *394*, 780–784. 10.1038/29528, PubMed: 9723616

Hohl S. S., Chaisanguanthum, K., & Lisberger, S. G. (2013). Sensory population decoding for visually guided movements. *Neuron*, *79*, 167–179. 10.1016/j.neuron.2013.05.026, PubMed: 23849202

Huang, X., & Lisberger, S. G. (2009). Noise correlations in cortical area MT and their potential impact on trial-by-trial variation in the direction and speed of smooth pursuit eye movements. *J. Neurophysiol.*, *101*, 3012–3030. 10.1152/jn.00010.2009, PubMed: 19321645

Kalidindi, H. T., Cross, K. P., Lillicrap, T. P., Omrani, M., Falotico, E., Sabes, P. N., & Scott, S. H. (2021). Rotational dynamics in motor cortex are consistent with a feedback controller. *eLife*, *10*, e67256. 10.7554/eLife.67256, PubMed: 34730516

Kase, M., Noda, H., Suzuki, D. A., & Miller, D. C. (1979). Target velocity signals of visual tracking in vermal Purkinje cells of the monkey. *Science*, *205*, 717–720. 10.1126/science.111350, PubMed: 111350

Krauzlis, R. J., & Lisberger, S. G. (1989). A control systems model of smooth pursuit eye movements with realistic emergent properties. *Neural Computation*, *1*, 116–122. 10.1162/neco.1989.1.1.116

Krekelberg, B., van Wezel, R. J., & Albright, T. D. (2006). Interactions between speed and contrast tuning in the middle temporal area: Implications for the neural code for speed. *J. Neurosci.*, *26*, 8988–8998. 10.1523/JNEUROSCI.1983-06.2006, PubMed: 16943555

Kurkin, S., Akao, T., Fukushima, J., Shichinohe, N., Kaneko, C. R., Belton, T., & Fukushima K. (2014). No-go neurons in the cerebellar oculomotor vermis and caudal fastigial nuclei: Planning tracking eye movements. *Exp. Brain Res.*, *232*, 191–210. 10.1007/s00221-013-3731-x, PubMed: 24129645

Lisberger, S. G. (2010). Smooth pursuit eye movements: Sensation, action, and what happens in between. *Neuron*, *66*, 477–491. 10.1016/j.neuron.2010.03.027, PubMed: 20510853

Lisberger, S. G. (2015). Visual guidance of smooth pursuit eye movements. *Ann. Rev. Vis. Sci.*, *1*, 447–468. 10.1146/annurev-vision-082114-035349

Lisberger, S. G., & Fuchs, A. F. (1978). Role of primate flocculus during rapid behavioral modification of vestibulo-ocular reflex. I. Purkinje cell activity during visually guided horizontal smooth pursuit eye movements and passive head rotation. *J. Neurophysiol.*, *41*, 733–763. 10.1152/jn.1978.41.3.733, PubMed: 96225

Lisberger, S. G., & Movshon, J.A. (1999). Visual motion analysis for pursuit eye movements in area MT of macaque monkeys. *J. Neurosci.*, *19*, 2224–2246. 10.1523/JNEUROSCI.19-06-02224.1999, PubMed: 10066275

Lisberger, S. G., & Westbrook, L. E. 1985. Properties of visual inputs that initiate horizontal smooth pursuit eye movements in monkeys. *J. Neurosci.*, *5*, 1662–1673. 10.1523/JNEUROSCI.05-06-01662.1985, PubMed: 4009252

Luebke, A. E., & Robinson, D. A (1988). Transition dynamics between pursuit and fixation suggest different systems. *Vision Res.*, *28*, 941–946. 10.1016/0042-6989(88)90103-4, PubMed: 3250089

Medina, J. F., & Lisberger, S. G. (2007). Variation, signal, and noise in cerebellar sensory-motor processing for smooth pursuit eye movements. *J. Neurosci.*, *27*, 6832–6842. 10.1523/JNEUROSCI.1323-07.2007, PubMed: 17581971

Morris, E. J., & Lisberger, S. G. (1987). Different responses to small visual errors during initiation and maintenance of smooth pursuit eye movements in monkeys. *J. Neurophysiol.*, *58*, 1351–1369. 10.1152/jn.1987.58.6.1351, PubMed: 3437336

Orban de Xivry, J.-J., Coppe, S., Blohm, G., & Lefevre P. (2013). Kalman filtering naturally accounts for visually guided and predictive smooth pursuit dynamics. *J. Neurosci.*, *33*, 17301–17313. 10.1523/JNEUROSCI.2321-13.2013, PubMed: 24174663

Osborne, L. C., Lisberger, S. G., & Bialek, W. (2005). A sensory source for motor variation. *Nature*, *437*, 412–416. 10.1038/nature03961, PubMed: 16163357

Pack, C. C., Hunter, J. N., & Born, R. T. (2005). Contrast dependence of suppressive influences in cortical area MT of alert macaque. *J. Neurophysiol.*, *93*, 1809–1815. 10.1152/jn.00629.2004, PubMed: 15483068

Priebe, N., Churchland, M., & Lisberger, S. G. (2001). Reconstruction of target speed for the guidance of pursuit eye movements. *J. Neurosci.*, *21*, 3196–3206. 10.1523/JNEUROSCI.21-09-03196.2001, PubMed: 11312304

Priebe, N. J., & Lisberger, S. G. (2004). Estimating target speed from the population response in visual area MT. *J. Neurosci.*, *24*, 1907–1916. 10.1523/JNEUROSCI.4233-03.2004, PubMed: 14985431

Rashbass, C. (1961). The relationship between saccadic and smooth tracking eye movements. *J. Physiol.*, *159*, 326–338. 10.1113/jphysiol.1961.sp006811, PubMed: 14490422

Ringach, D. L. (1995). A "tachometer" feedback model of smooth pursuit eye movements. *Biol. Cybern.*, *73*, 561–568. 10.1007/BF00199548, PubMed: 8527501

Robinson, D. A (1965). The mechanics of human smooth pursuit eye movement. *J. Physiol. (London)*, *180*, 569–591. 10.1113/jphysiol.1965.sp007718

Robinson, D. A, Gordon, J. L., & Gordon, S. E. (1986. A model of the smooth pursuit eye movement system. *Biol. Cybern.*, *55*, 43–57. 10.1007/BF00363977, PubMed: 3801529

Schoppik, D., Nagel, K. I., & Lisberger, S. G. (2008). Cortical mechanisms of smooth eye movements revealed by dynamic covariations of neural and behavioral responses. *Neuron*, *58*, 248–260. 10.1016/j.neuron.2008.02.015, PubMed: 18439409

Schwartz, J. D., & Lisberger, S. G. (1994). Modulation of the level of smooth pursuit activation by initial tracking conditions in monkeys. *Visual Neuroscience*, *11*, 411–424. 10.1017/S0952523800002352, PubMed: 8038118

Shenoy, K. V., Sahani, M., & Churchland, M. M. (2013). Cortical control of arm movements, a dynamical systems perspective. *Annu. Rev. Neurosci.*, *36*, 337–359. 10.1146/annurev-neuro-062111-150509, PubMed: 23725001

Stone, L. S., & Lisberger, S. G. (1990). Visually-driven output from the primate flocculus. I. Simple-spike responses to the visual inputs that initiate pursuit eye movements. *J. Neurophysiol.*, *63*, 1241–1261. 10.1152/jn.1990.63.5.1241, PubMed: 2358872

Tanaka, M., & Lisberger, S. G. (2001). Regulation of the gain of visually-guided smooth pursuit eye movements by frontal cortex. *Nature*, *409*, 191–194. 10.1038/35051582, PubMed: 11196642

Tanaka M., & Lisberger, S. G. (2002). Role of arcuate frontal cortex of monkeys in smooth pursuit eye movements. I. Basic response properties to retinal image motion and position. *J. Neurophysiol.*, *87*, 2684–2699. 10.1152/jn.2002.87.6.2684, PubMed: 12037171

Yang, J., Lee, J., &Lisberger, S. G. (2012). The interaction of Bayesian priors and sensory data and its neural circuit implementation in visually-guided movement. *J. Neurosci.*, *32*, 17632–17645. 10.1523/JNEUROSCI.1163-12.2012, PubMed: 23223286

Received February 2, 2022; accepted March 31, 2022.